Machine Learning of Optimal Processing Conditions in Ultrafast Laser Welding of Glass Based on Laser Emission State

Shun Irie [*1], Wataru Watanabe [2], and Takayuki Tamaki [1]

1- Advanced Mechanical Engineering Course, Department of Systems Innovation, Faculty of Advanced Engineering, National Institute of Technology (KOSEN), Nara College, Japan
2- Department of Electrical & Electronic Engineering, College of Science and Engineering, Ritsumeikan University, Japan
** Corresponding author's e-mail: am1160@nara.kosen-ac.jp*

In this study, we developed a machine-learning framework to predict the success of ultrafast laser microwelding of glass substrates based on plasma-emission spectra and laser-processing parameters. Ten-millimetre linear welds were produced under varying laser power, repetition rate, and scanning speed. The emission spectra collected during welding, combined with the corresponding processing conditions, were used to train support vector machine (SVM) and neural network (NN) classifiers. Both models demonstrated strong predictive performance, achieving over 80% accuracy on test data. Although a slight decrease in accuracy was observed on newly acquired data, this result highlights the potential for further improvement through data diversification. By expanding the dataset and incorporating environmental factors such as temperature and humidity, we aim to enhance the robustness and generalisation capability of the models. This approach offers a promising path toward improving the reliability and efficiency of ultrafast laser microwelding processes.

DOI: 10.2961/jlmn.2026.01.2010
Keywords: machine learning, ultrafast laser microwelding, support vector machine, neural network, femtosecond laser, glass

1. Introduction

Laser processing is a non-contact energy delivery method that enables highly precise and controllable machining. Its strong compatibility with numerical control (NC) systems has accelerated adoption across fields ranging from automotive manufacturing to electronics and medical devices. By selecting an appropriate laser type, wavelength, and pulse duration, laser processing can accommodate a wide variety of materials and applications, making it especially attractive for high-value microfabrication.

This study focuses on femtosecond laser processing, which employs ultrashort pulses on the order of 10^{-15} s. Because the interaction time is extremely brief, femtosecond lasers minimize thermal loading and greatly reduce side effects such as thermal deformation, cracking, and melting. As a result, they enable high-precision machining even for difficult-to-process materials, such as brittle substrates and ultra-hard alloys.

One particularly promising application is the welding of transparent materials such as glass. Conventional methods usually require intermediate absorbing layers to match the laser wavelength. Recent advances in ultrafast laser microwelding eliminate this requirement by tightly focusing femtosecond or picosecond pulses at the interface between two transparent substrates. Non-linear effects—multiphoton absorption and tunnelling ionization—produce localized melting, and subsequent resolidification creates a direct bond [1].

This technique is well suited to optical components and microfluidic devices, where highly localized and precise bonds are essential. Achieving consistent quality, however, remains challenging because material properties such as melting point, thermal conductivity, and optical transmittance vary among substrates. Even under identical processing conditions, satisfactory results are not guaranteed. Key parameters—including pulse energy, repetition rate, wavelength, pulse duration, numerical aperture of the focusing lens, and scan speed—significantly influence the welding outcome.

To address these challenges, Fujiwara *et al.* investigated optical emission near the focal point during glass welding and proposed a method for evaluating the welding state. By extracting video frames at regular intervals and analyzing their RGB values, they showed that variations in the blue component correlate with melting, while the temporal emission profile depends on interfacial conditions such as the glass-to-air ratio [2].

In recent years, machine learning techniques have been increasingly employed in the field of laser processing [3-5]. Furthermore, several studies have investigated the evaluation of welding quality by analyzing the optical emission spectra of plasma generated during the processing [6].

Building on this foundation, the present study combines plasma-emission spectra with laser processing parameters—average power, repetition rate, pulse duration, scan speed, and ambient pressure—and analyzes them using machine learning. This data-driven approach aims to reduce trial and error in parameter selection and to realize a more stable, efficient ultrafast laser microwelding process.

2. Methodology

2.1 Experimental setup and materials

The optical system used in this experiment is illustrated in Figure 1. The laser beam emitted from the source was directed through a series of optical components, including a mirror, a half-wave plate, a polarizer, and an objective lens (10× magnification, NA (numerical aperture) = 0.25), before being focused onto the sample. The laser output was controlled using the half-wave plate and polarizer, and the average power was measured with a power meter. A spectrometer was installed to monitor the optical emission generated during the laser microwelding process.

The spectrometer was capable of detecting wavelengths ranging from 339.59 nm to 1023.98 nm, with a spectral resolution of 0.38 nm.

To securely hold the glass substrates during processing, a custom-designed jig was employed. This jig, actuated by an air cylinder, applied pressure to the two glass substrates during welding. A schematic diagram of the jig is presented in Figure 2. The glass substrates used in this study were made of SCHOTT B270 glass, with dimensions of 50 mm × 50 mm and a thickness of 1 mm. The thickness of the glass was first measured using a caliper with a resolution of 50 µm. Subsequently, the glass was placed in the jig and clamped using an air cylinder, after which the combined thickness of the glass and the jig was measured. The thickness of the jig in this measurement was 3.50 mm. The results are summarized in Tables 1 and 2.

From these results, it can be concluded that no gap larger than 50 µm was present.

The interference fringes were observed under white-light illumination, and the images were recorded through a 520 nm bandpass filter (FWHM (full width at half maximum) = 35 nm).

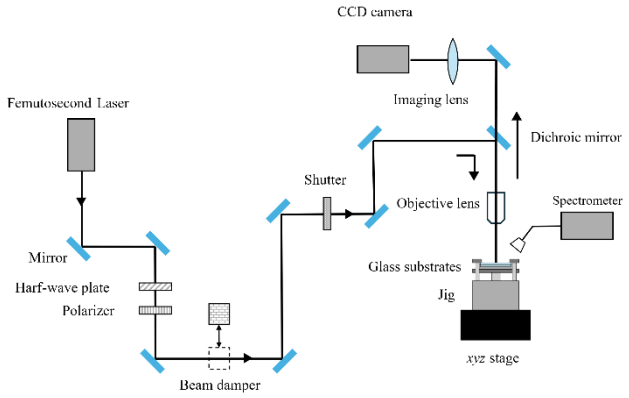

Fig. 1 Schematic of the optical setup for ultrafast laser microwelding and measurement of plasma-emission spectra.

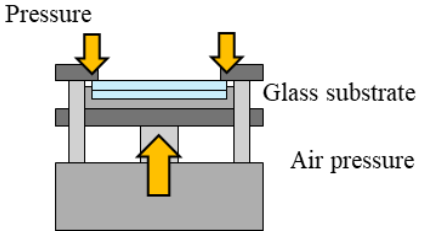

Fig. 2 Schematic of the air-cylinder-actuated jig used to press the glass substrates during welding.

Five photographs were taken, and the images were post-processed to enhance the visibility of the interference fringes.

Assuming the light to have a wavelength of 520 nm, the optical path difference corresponding to one wavelength is 520 nm. Therefore, the spacing between adjacent fringes corresponds to half of this value, i.e., 260 nm.

In the case with the largest number of fringes, shown in Fig. 3(a), ten fringes can be observed from the center toward the edge. Accordingly, the optical path difference is estimated to be 260 × 10 = 2600 nm, indicating that the maximum gap between the glass substrates is approximately 2.6 µm.

For Fig. 3(d), six fringes are observed, corresponding to an optical path difference of 260 × 6 = 1560 nm, i.e., a gap of approximately 1.56 µm.

To adjust the focus, an approximate focal position was first obtained, after which the height was varied in 10 µm increments. The welding experiments were then conducted at the central position within the range where successful bonding was achieved. These procedures ensured that the experiments were carried out under stable and reproducible conditions.

2.2 Experimental Procedure

The welding conditions used in this study are described below. Two glass substrates were fixed in the custom jig described above and compressed at a pressure of 0.225 MPa. The laser beam was focused at the interface between the two glass substrates, and linear welding was performed by translating the stage over a distance of 10 mm while irradiating the sample.

The laser used in the experiment had a wavelength of 1030 nm and a pulse duration of 190 fs. The average power, repetition rate, and scanning speed were varied as shown in Table 3, resulting in 120 different parameter combinations. Each condition was tested twice, yielding a total of 240 welding trials. During each welding process, optical emission spectra were recorded using a spectrometer. For each

Table 1 The thickness of the glass.

Sample number	Thickness [mm]
1	1.00
2	1.00
3	1.00
4	1.00
5	1.00
6	1.00
7	1.00
8	1.00
9	1.00
10	1.00

Table 2 Thickness of the glass after being clamped in the jig and pressed with the air cylinder.

Sample number	Thickness [mm]
1-2	5.50
3-4	5.50
5-6	5.50
7-8	5.50
9-10	5.50

sample, 20 spectra were acquired per welding operation.

Welding success was determined based on two primary criteria. The first was the formation of Newton's rings on the welded sample. Newton's rings are interference fringes that appear at the interface between two flat glass surfaces due to optical interference. When the contact between the substrates is sufficiently close, the air gap becomes thin enough to allow interference, resulting in concentric or striped fringe patterns. The clear presence of Newton's rings indicates minimal interfacial voids and intimate bonding, and thus serves as an indicator of successful welding.

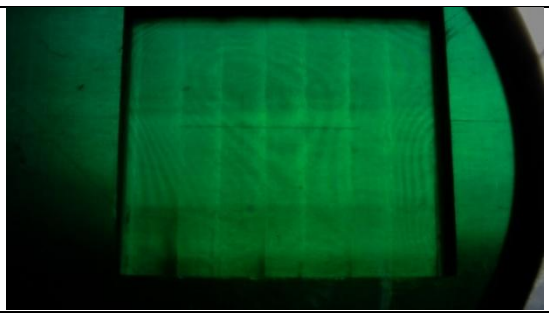

(a) 1-2

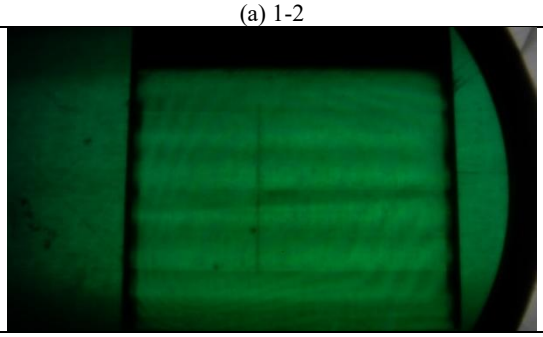

(b) 3-4

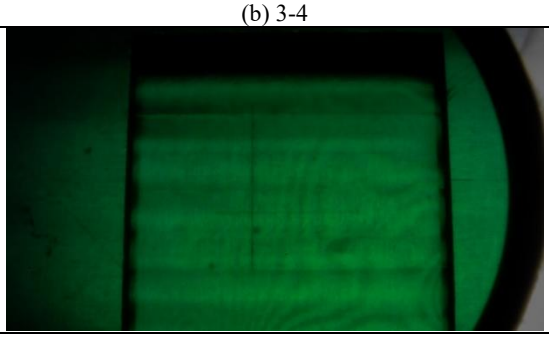

(c) 5-6

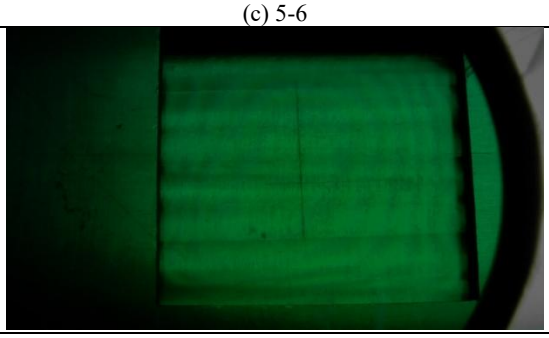

(d) 7-8

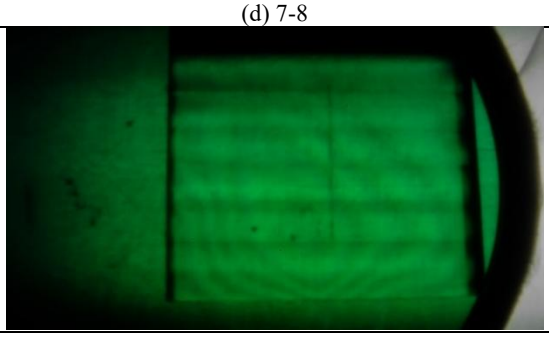

(e) 9-10

Fig. 3 Interference fringes in the stacked glass.

The second criterion was the presence or absence of delamination when a small external force was applied to the bonded region. Specifically, the sample was gently pressed by hand to observe whether the bonded interface separated or shifted. If the bonding strength was insufficient, even a light manual force could cause delamination. In contrast, a bond with adequate mechanical strength would remain intact under such conditions. A welding trial was considered "successful" only when both of these criteria were satisfied.

To obtain a reference for the mechanical strength of the welds, shear force measurements were conducted on the samples welded under two extreme parameter sets selected from the 240 conditions:

- The condition that produced the longest actual welded length (1.5 W, 590 kHz, 1.5 mm/s), and
- The condition that produced the shortest actual welded length (1.2 W, 590 kHz, 0.25 mm/s).

For each condition, three samples were prepared. The welded glass samples were mounted on a mechanical testing apparatus, and shear force was measured using a digital force gauge while the electric stage was moved at a constant speed of 2 mm/s (Fig. 4 and Fig. 5).

2.3 Machine learning

To minimize the influence of non-plasma-related emissions, the spectra obtained during the welding process were baseline-corrected by subtracting the spectra measured under conditions with no plasma emission. Using the corrected spectra, we constructed a dataset consisting of

Table 3 Processing conditions.

Wavelength [nm]	1030
Pulse width [fs]	190
NA	0.25
Spot diameter [μm]	5
Power [W]	0.5, 0.75, 1.0, 1.2, 1.5, 1.75
Repetition rate [Hz]	100 k , 200 k , 590 k , 1 M
Scanning speed [mm/s]	0.1, 0.25, 0.5, 1.0, 1.5

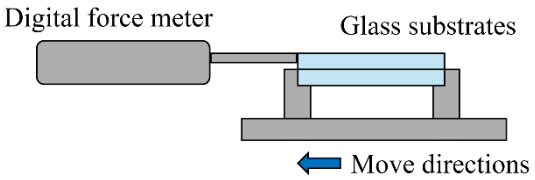

Fig. 4 Method for measuring shear force.

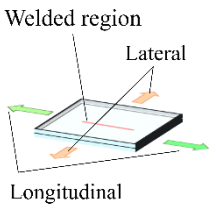

Fig. 5 Direction of shear force.

approximately 20 spectra per welding trial for all 240 welding conditions (120 parameter sets, each repeated twice). Each spectrum was paired with its corresponding processing parameters: average power, repetition rate, pulse energy, scanning speed, and applied pressure.

The dataset was randomly divided into training and testing subsets, with 70% used for training and 30% used for testing. Machine learning models were then trained to predict whether the welding was successful or not based on these input features.

Two algorithms were employed in this study: Support Vector Machine (SVM) and Neural Network (NN). The SVM is a supervised learning algorithm that is particularly effective for classification tasks and can model nonlinear relationships using kernel functions. The NN model used here was a feedforward neural network consisting of an input layer with 2,025 units, followed by two hidden layers with 128 and 64 units respectively, and a single-unit output layer for binary classification.

All machine learning models were implemented in Python 3.11.12. The SVM was developed using the scikit-learn library, whereas the NN was constructed with tensorflow.keras, with data preprocessing carried out using scikit-learn. To mitigate overfitting, an early stopping strategy was incorporated during the NN training process. Model development and training were performed in the Google Colab environment.

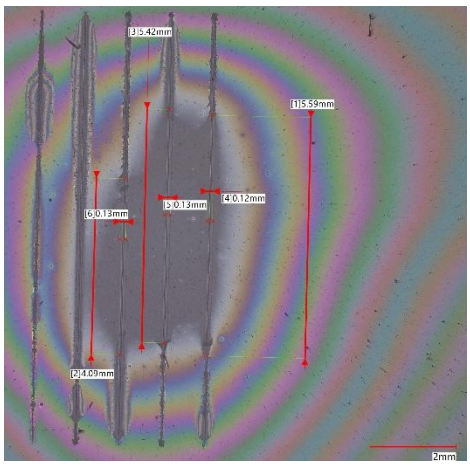

Fig. 6 Optical microscope image showing representative welding results obtained under multiple processing conditions.

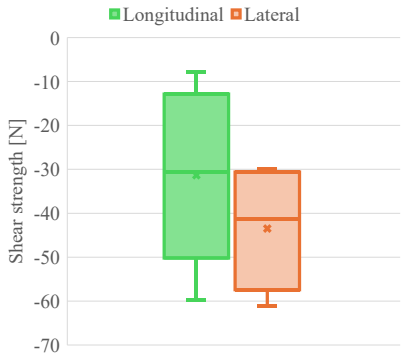

Fig. 7 Comparison of shear force for welds produced under the conditions yielding the longest and shortest welded lengths.

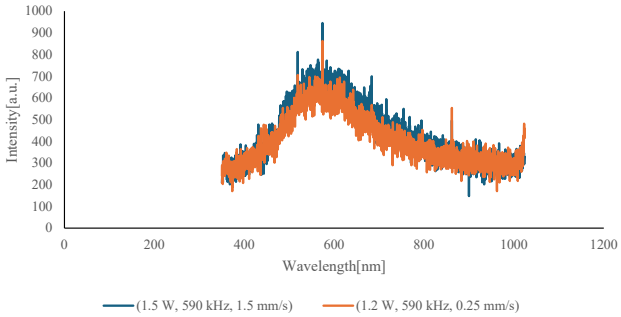

Fig. 8 The measured spectra

3. Results

3.1 Welding results

An example of welding outcomes obtained under multiple processing conditions is shown in Fig. 6. In this case, the laser parameters were fixed at 1.2 W and 1 MHz, while the scanning speeds was varied across 0.1, 0.25, 0.5, 1.0, and 1.5 mm/s. The corresponding shear force measurements in different loading directions are shown in Fig. 7.

As illustrated in Fig. 6, clear Newton's rings were observed, indicating that successful welding was achieved. According to the shear strength results, the average joint strength in the longitudinal direction was approximately –30 N, while in the lateral direction it exceeded –40 N. These findings suggest that the joint strength was higher when the load was applied laterally. Note that in this context the negative sign denotes that the applied force acts in the opposite direction (rightward) when the leftward direction is defined as positive in the coordinate system.

3.2 Machine learning

The measured spectra are shown in Fig. 8. The experimental conditions correspond to the longest actual welded seam obtained (1.5 W, 590 kHz, 1.5 mm/s) and to the shortest actual welded seam obtained (1.2 W, 590 kHz, 0.25 mm/s). Figures 9 and 10 present the confusion matrices and the evaluation metrics used to assess the performance of the trained models on the test dataset. The number of epochs until convergence for the NN training was 61, as determined by the early stopping criterion. A brief explanation of the evaluation metrics employed in this study is provided below:

Accuracy refers to the proportion of all predictions that were correctly classified. It is the most fundamental metric for evaluating overall model performance. However, in cases where the dataset is imbalanced, accuracy alone may not adequately reflect the true effectiveness of the model and should therefore be interpreted alongside other metrics.

Precision indicates the proportion of instances predicted as positive (*i.e.*, "successful welding") that were actually positive. It reflects the reliability of the model's positive predictions. A higher precision value implies fewer false positives and greater confidence in the model's output.

Recall (also known as sensitivity) measures the proportion of actual positive instances that were correctly identified by the model. A higher recall indicates a lower likelihood of missing successful welds, which is particularly

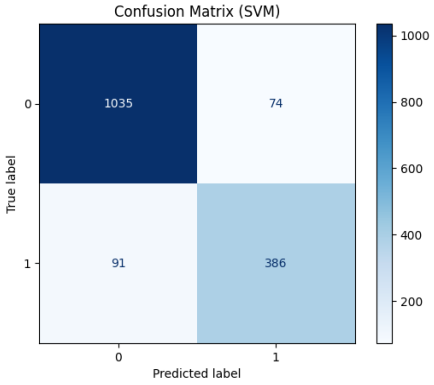

	Precision	Recall	F1-score
Not joinable	0.92	0.93	0.93
Joinable	0.84	0.81	0.82
Accuracy			0.90

Fig. 9 Confusion matrix and evaluation metrics of the SVM model on the test dataset.

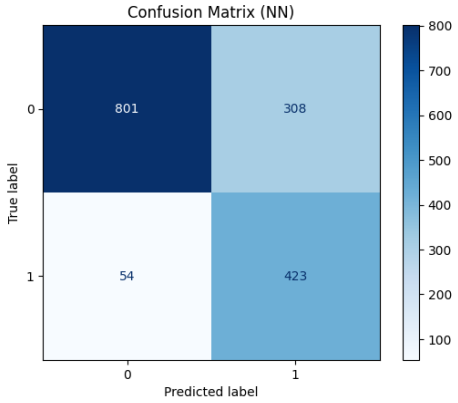

	Precision	Recall	F1-score
Not joinable	0.94	0.72	0.82
Joinable	0.58	0.89	0.70
Accuracy			0.77

Fig. 10 Confusion matrix and evaluation metrics of the NN model on the test dataset.

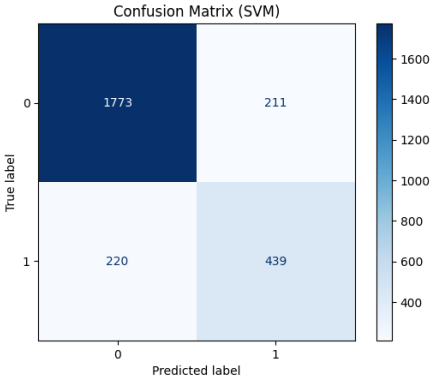

	Precision	Recall	F1-score
Not joinable	0.89	0.89	0.89
Joinable	0.68	0.67	0.67
Accuracy			0.84

Fig. 11 Confusion matrix and evaluation metrics of the SVM model on another dataset.

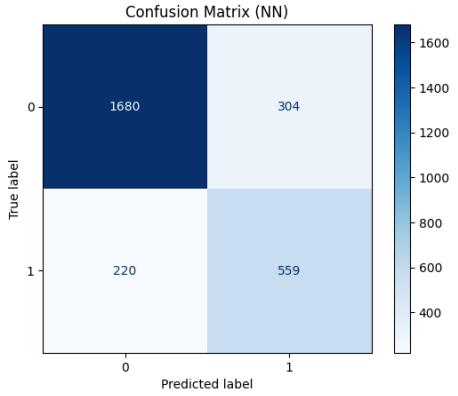

	Precision	Recall	F1-score
Not joinable	0.94	0.85	0.89
Joinable	0.65	0.85	0.73
Accuracy			0.85

Fig. 12 Confusion matrix and evaluation metrics of the NN model on another dataset

important in applications where safety or quality is critical.

F1-score is the harmonic mean of precision and recall. It provides a balanced evaluation that penalizes models with high precision but low recall (or vice versa). This metric is particularly useful when dealing with class imbalance or when the cost of different types of misclassification varies between classes.

By collectively evaluating accuracy, precision, recall, and F1-score, we were able to comprehensively assess how accurately and reliably each model could predict welding outcomes.

The two machine learning models developed in this study—Support Vector Machine (SVM) and Neural Network (NN)—were compared based on these metrics.

The SVM model achieved high values (≥0.80) across all four evaluation metrics, indicating excellent overall classification performance. Notably, both precision and recall remained consistently high, demonstrating that the model maintained a favorable balance between prediction reliability and detection sensitivity.

In contrast, the NN model achieved a comparable level of accuracy to that of the SVM; however, its precision was somewhat lower, suggesting reduced reliability in predicting successful welding outcomes and higher incidence of false positives. Nevertheless, the NN exhibited higher recall than the SVM, indicating a lower likelihood of missing actual successful welds—an advantage in applications where minimizing oversight is critical.

In summary, both the SVM and NN models demonstrated sufficient predictive capability, confirming their usefulness for predicting the success or failure of ultrafast laser microwelding processes.

3.3 Validation with experimental data

To evaluate the generalizability of the developed models, we tested them on a separate set of 120 newly acquired experimental data samples. The corresponding confusion matrix and evaluation metrics for this validation are presented in Fig. 10 and Fig. 11, respectively.

As shown in Fig. 10 and Fig. 11, both models maintained a high level of overall classification performance, as indicated by the accuracy metric. However, in terms of the model's ability to correctly identify samples that should be classified as "successful welding"—as reflected by recall—the neural network (NN) model demonstrated a relatively better performance than the support vector machine (SVM).

In contrast, the precision values for both models were nearly equivalent and remained at a moderate level, suggesting that the reliability of positive predictions—i.e., the proportion of predicted successful welds that were actually successful—was limited. This indicates that while the models were capable of correctly identifying many successful cases, a substantial number of false positives remained.

Nonetheless, the relatively high recall of the NN model implies that it is more effective at detecting actual successful welding events without overlooking them. This highlights its potential utility in applications where failing to detect true positive could have critical consequences.

4. Discussion

In this study, we proposed and validated a machine learning-based approach to predict the success or failure of ultrafast laser microwelding by utilizing plasma emission spectra generated during the process, in combination with laser processing parameters. Although the trained models achieved high prediction accuracy on the test dataset, their performance declined noticeably when evaluated on newly acquired experimental data.

One primary factor contributing to this decline in the limited size and diversity of the training dataset. In machine learning, a sufficiently large and varied dataset is essential for enhancing a model's generalization capability. This is especially important in complex systems involving multiple interdependent variables such as laser power, scanning speed, applied pressure, and emission spectra. Capturing the full range of variability in such multidimensional relationships requires a broader and more comprehensive dataset.

Another factor that may have affected model performance is the temporal gap between the acquisition of the training and test data. It is well known that laser processing is highly sensitive to external conditions, including ambient temperature, humidity, equipment stability, and even minor changes in the optical path. As a result, even under identical parameter settings, the intensity and shape of the emission spectra may vary depending on environmental conditions at the time of measurement, potentially leading to prediction errors.

5. Conclusion

In this study, we aimed to explore optimal conditions for ultrafast laser microwelding of glass substrates by analyzing plasma emission spectra and corresponding laser parameters using machine learning techniques.

The results demonstrated that our models achieved high classification performance on the test dataset, with an accuracy exceeding 80%, indicating strong predictive capability during the training phase. However, when applied to newly acquired experimental data a significant drop in precision was observed, revealing limitations in the model's reliability under varying experimental conditions.

This discrepancy is likely attributable to several factors, including environmental fluctuations during experimentation, dataset bias, and potential model overfitting. To address these issues, future efforts will focus on expanding the dataset to cover a broader range of conditions and incorporating environmental parameters such as temperature and humidity. These enhancements are expected to improve both the generalization ability and robustness of the predictive models in real-world applications.

In addition, we plan to extend the model's capabilities beyond binary classification of welding success, to enable prediction of quantitative quality metrics such as weld length and shear force.

These advancements will enhance the practical applicability of our approach and contribute to the further development of ultrafast laser microwelding technology, ultimately facilitating the realization of intelligent, adaptive process control systems.

Acknowledgments

This work was supported by JSPS KAKENHI Grant Number 25K07521.

References

[1] W. Watanabe and T. Tamaki: J. Jpn. Soc. Precis. Eng., 81, (2015) 731.
[2] J. Fujiwara, H. Okuno, T. Sasahara, T. Ota, W. Watanabe, and T. Tamaki: J. Laser Micro Nanoeng., 19, (2024) 145.
[3] M.D.T. McDonnell, D. Arnaldo, E. Pelletier, J.A. Grant Jacob, M. Praeger, D. Karnakis, R.W. Eason, and B. Mills: J. Intell. Manuf., 32, (2021) 1471.
[4] T. Kusumoto: J. Laser Soc. Jpn., 50, (2022) 142.
[5] Y.-M. Ho, C.-H. Lee, J.-R. Ho, C.-K. Lin, P.-C. Tung, and Y.-S. Lee: Manuf. Lett., 35, (2023) 160.
[6] T. Sibillano, A. Ancona, V. Berardi, and P.M. Lugarà: Sensors, 9, (2009) 3376.
[7] K. Cvecek, S. Dehmel, I. Miyamoto, and M. Schmidt: Int. J. Extrem. Manuf., 1, (2019) 042001.
[8] S. Raschka and V. Mirjalili: "Python Machine Learning, 3rd Edition", trans. by Quipu Inc., supervised by S. Fukushima, (Impress, Tokyo, 2020).
[9] Y. Matsuo: J. Plasma Fusion Res., 80, (2004) 777.

(Received: June 30, 2025, Accepted: January 10, 2026)